NLO QCD Corrections for Higgs Production via Weak-Boson Fusion

Terrance Figy
Phenomenology Institute,
University of Wisconsin -Madison

Loopfest III
April 1,2004
In collaboration with:
D. Zeppenfeld and C. Oleari

- Introduction
- The NLO QCD calculation
- Tagging Jet Properties at NLO
- Jet Correlations
- Conclusions

Introduction

The WBF process $qQ \to qQH$ is expected to provide a copious source of Higgs bosons at the CERN LHC.

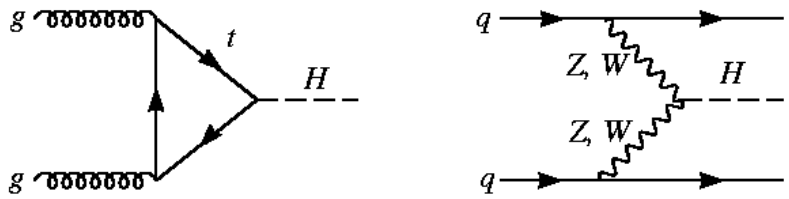

(a) (b)

Together with gluon fusion, WBF represents the most promising production process for Higgs boson discovery.

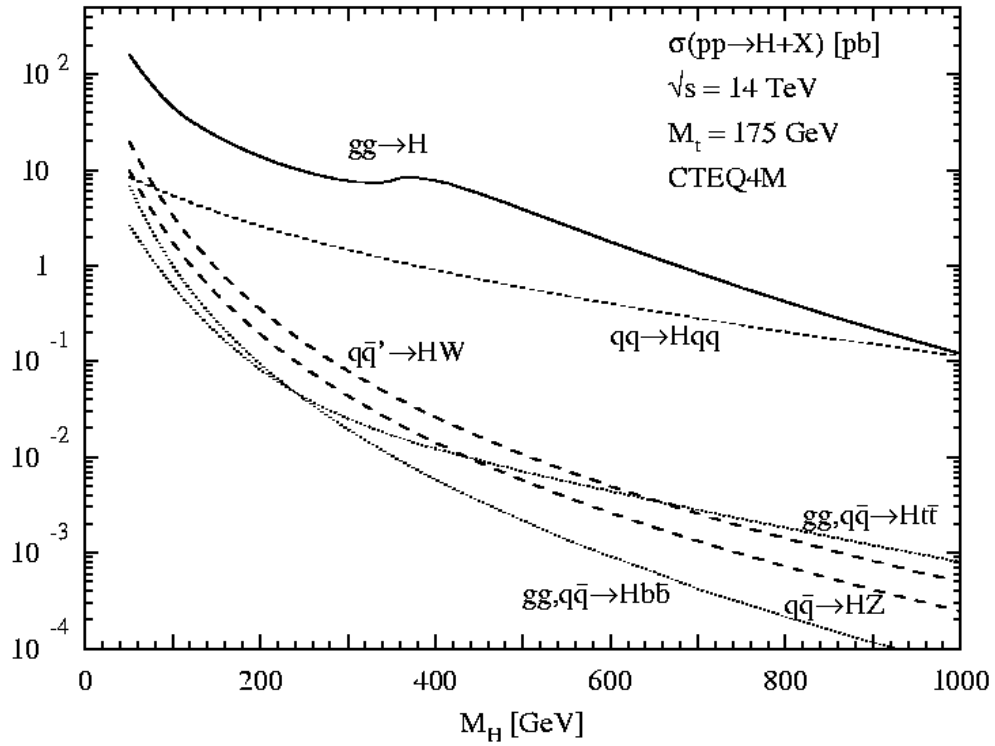

Spira and Zeras (hep-ph/9803257)

WBF is of central importance since it allows a precise coupling measurement of the HWW and HZZ vertex interactions. This includes the vertex tensor structure.

These measurements can be performed at the LHC with statistical accuracies on the $\sigma \cdot B$ of order $10 - 20\%$.

In order to extract the Higgs boson coupling constants with this full statistical power, a theoretical prediction of the SM production cross section with an error well below 10% is required.

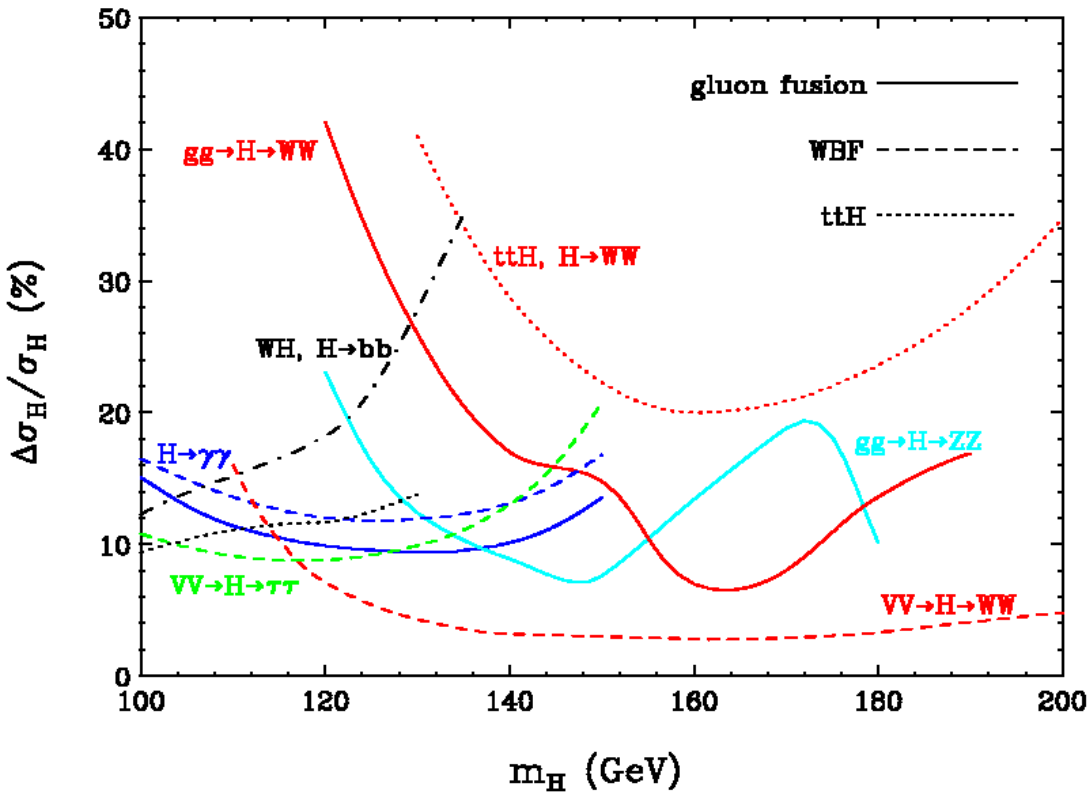

D.Zeppenfeld (hep-ph/0203123)

Distinguishing the WBF Higgs boson signal from backgrounds requires cuts on both the decay products as well as the two forward quark jets.

Typical cuts have an acceptance of less than 25% of the starting value for $\sigma \cdot B$.

Are the K-factors and the scale dependence* ,determined for the inclusive production cross section, valid in the Higgs boson search region?

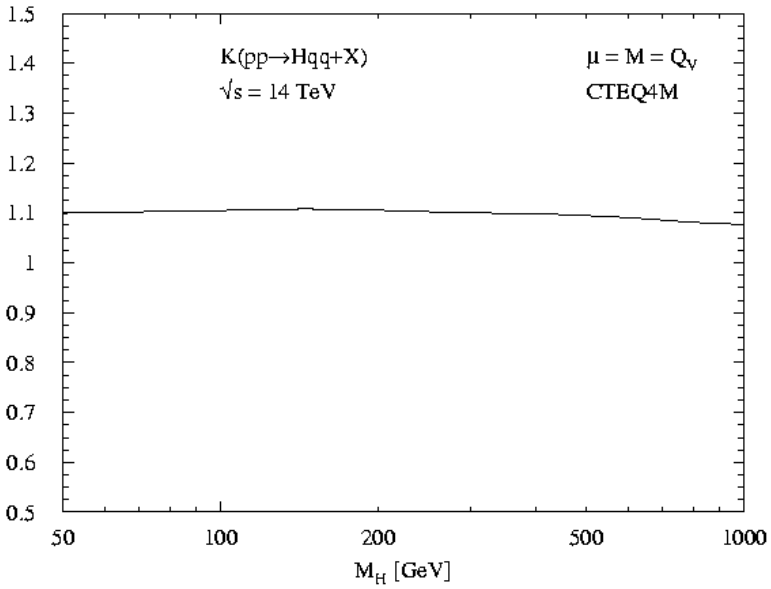

Spira

To address this question, we † have implemented the one-loop QCD corrections to WBF in a fully flexible NLO parton-level Monte Carlo program.

*T. Han, G. Valencia and S. Willenbrock, Phys. Rev. Lett. **69**, 3274 (1992)

†T.Figy,C.Oleari,D.Zeppenfeld,Phys.Rev.D68,073005(2003)

LO and NLO virtual diagrams

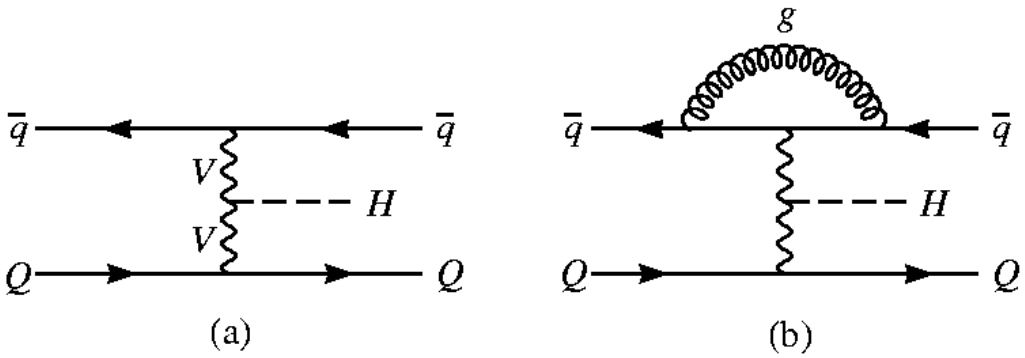

NLO: real diagrams

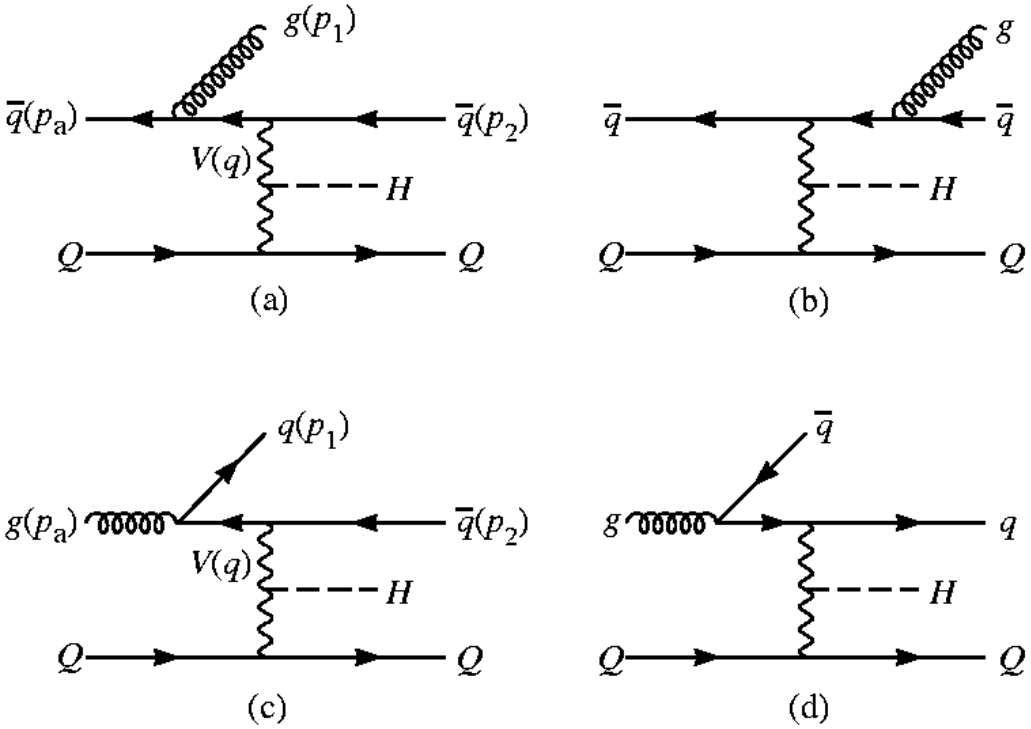

NLO Calculation

We use the subtraction method of Catani and Seymour*.

The Regularization: The virtual correction amplitude $\mathcal{M}_V$ is:

$$2\,\mathrm{Re}\left[\mathcal{M}_V\mathcal{M}_B^*\right] = |\mathcal{M}_B^{\bar{q}}|^2 \frac{\alpha_s(\mu_R)}{2\pi} C_F \left(\frac{4\pi\mu_R^2}{Q^2}\right)^{\epsilon} \Gamma(1+\epsilon)\left[-\frac{2}{\epsilon^2} - \frac{3}{\epsilon} + c_{\mathrm{virt}}\right] .$$

In dimensional reduction this contribution is given by $c_{\mathrm{virt}} = \pi^2/3 - 7$ ($c_{\mathrm{virt}} = \pi^2/3 - 8$ in conventional dimensional regularization).

The $1/\epsilon$ and $1/\epsilon^2$ poles in $2\,\mathrm{Re}\left[\mathcal{M}_V\mathcal{M}_B^*\right]$ cancel against those in the real emission subtraction terms and the collinear counter terms.

$$< \mathbf{I}(\epsilon) >= |\mathcal{M}_B^{\bar{q}}|^2 \frac{\alpha_s(\mu_R)}{2\pi} C_F \left(\frac{4\pi\mu_R^2}{Q^2}\right)^{\epsilon} \Gamma(1+\epsilon)\left[\frac{2}{\epsilon^2} + \frac{3}{\epsilon} + 9 - \frac{4}{3}\pi^2\right] .$$

*hep-ph/9605323

The three-parton NLO cross section:

$$\sigma_3^{NLO}(\bar{q}Q \to \bar{q}QHg) = \int_0^1 dx_a \int_0^1 dx_b\, f_{\bar{q}/p}(x_a,\mu_F)\; f_{Q/p}(x_b,\mu_F) \times \frac{1}{2\hat{s}}\, d\Phi_4(p_1,p_2,p_3,P;p_a+p_b) \times \left\{ \left|\mathcal{M}_r^{\bar{q}}\right|^2 F_J^{(3)}(p_1,p_2,p_3) - \left|\mathcal{M}^{\bar{q}}\right|^2_{\text{sing}} F_J^{(2)}(\tilde{p}_2,p_3) \right\},$$

The functions $F_J^{(3)}$ and $F_J^{(2)}$ define the jet algorithm for 3-parton and 2-parton final states. In the singular limits: $F_J^{(3)} \to F_J^{(2)}$

The two-parton NLO cross section:

$$\sigma_2^{NLO} = \int_0^1 dx_a \int_0^1 dx_b\, f_{\bar{q}/p}(x_a,\mu_F)\; f_{Q/p}(x_b,\mu_F) \times \frac{1}{2\hat{s}}\, d\Phi_3(p_2,p_3,P;p_a+p_b) \times \left|\mathcal{M}_B^{\bar{q}}\right|^2 F_J^{(2)}(p_2,p_3)\left[1+\frac{\alpha_s(\mu_{Ra})+\alpha_s(\mu_{Rb})}{2\pi} C_F\left(9-\frac{4}{3}\pi^2 c_{\text{virt}}\right)\right].$$

Finite collinear terms:

$$\sigma_{2,\text{coll}}^{NLO}(\bar{q}Q \to \bar{q}QH) = \int_0^1 dx_a \int_0^1 dx_b\, f^c_{\bar{q}/p}(x_a,\mu_F,\mu_{Ra})\; f_{Q/p}(x_b,\mu_F) \times \frac{1}{2\hat{s}}\, d\Phi_3(p_2,p_3,P;p_a+p_b)\; \left|\mathcal{M}_B^{\bar{q}}\right|^2 F_J^{(2)}(p_2,p_3),$$

These cross section contributions for $\bar{q}Q \to \bar{q}QH$ and crossing related channels have been implemented in a parton-level Monte Carlo program.

NLO Parton Monte Carlo Program

Tree-level amplitudes are calculated numerically, using helicity amplitude formalism.

CTEQ6M parton distributions with $\alpha_s(M_Z) = 0.118$ for all NLO results and CTEQ6L1 parton distributions for all leading order cross sections are used.

Identical fermion effects are neglected since these effects are suppressed by WBF cuts. We only consider t-channel W/Z exchanges.

In order to reconstruct jets from the final state partons, the k_T-algorithm with resolution parameter $D = 0.8$

For all Z-exchange contributions the b quark in included as an initial-and/or final-state massless parton. This contribution is about 3%.

Tagging Jet Properties at NLO

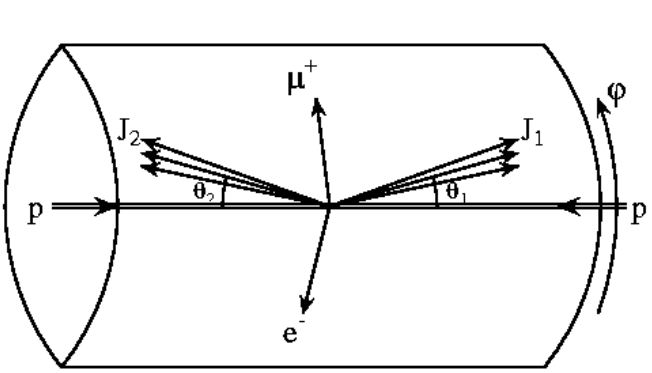

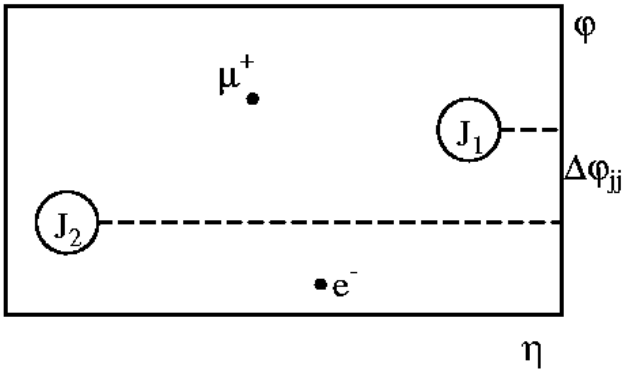

$$\eta = \frac{1}{2} \log \frac{1+\cos\theta}{1-\cos\theta}$$

Characteristics of WBF:

- energetic jets in the forward and backward directions ($p_T > 20$ GeV)
- Higgs decay products between tagging jets
- Little gluon radiation in the central-rapidity region, due to colorless W/Z exchange (central jet veto: no extra jets with $p_T > 20$ GeV and $|\eta| < 2.5$)

For the NLO corrections, cuts on Higgs boson decay products to play a minor role, with respect to WBF cuts.

The partonic cross sections are calculated for events with at least two hard jets,

$$p_{Tj} \geq 20 \text{ GeV}, \qquad |y_j| \leq 4.5.$$

y_j = rapidity of the (massive) jet momentum which is reconstructed as the four-vector sum of massless partons of pseudo-rapidity $|\eta| < 5$.

The Higgs boson decay products, called "leptons" (which represent $\tau^+\tau^-$ or $\gamma\gamma$ or $b\bar{b}$ final states) must satisfy

$$p_{T\ell} \geq 20 \text{ GeV}\,, \quad |\eta_\ell| \leq 2.5\,, \quad \Delta R_{j\ell} \geq 0.6\,,$$

where $R_{j\ell}$ denotes the jet-lepton separation in the rapidity-azimuthal angle plane. Additionally,

$$y_{j,min} < \eta_{\ell_{1,2}} < y_{j,max}\,.$$

All cross sections are $\sigma(hjj)$. Branching ratios are not included.

Consider two possibilities for selecting tagging jets:

"p_T-method"

the tagging jets are the two highest p_T jets in the event. This ensures that the tagging jets are part of the hard scattering event.

"E-method"

the tagging jets are the two highest energy jets in the event. This selection favors the very energetic forward jets which are typical for weak-boson fusion processes.

As a final requirement we employ the "rapidity gap cut".

$$\Delta y_{jj} = |y_{j_1} - y_{j_2}| > 4$$

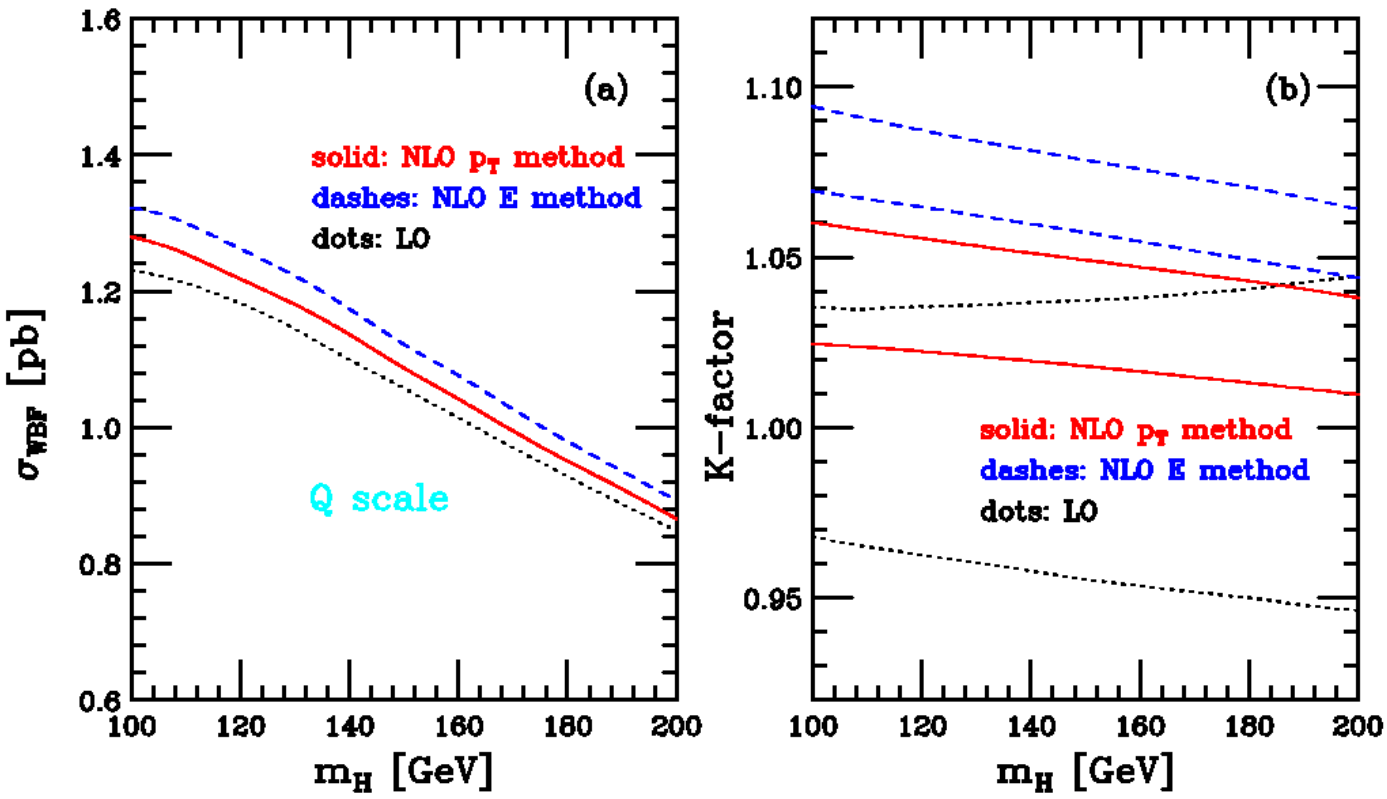

$$K = \frac{\sigma_{NLO}(\mu_R, \mu_F)}{\sigma_{LO}(\mu_F = Q)}$$

Two different scales to test scale dependence

$$\mu_F = \xi_F m_H \,, \qquad \mu_R = \xi_R m_H$$
$$\mu_{Fi} = \xi_F Q_i \,, \qquad \mu_{Ri} = \xi_R Q_i$$

Q_i = virtuality of the exchanged weak boson
(1 = upper line or 2 = lower line)

The largest scale variations occur when:

$$\xi = \xi_R = \xi_F \,, \qquad \xi = 1/2 \,, \qquad \xi = 2$$

Residual uncertainty:
±5% for LO and below ±2% for NLO

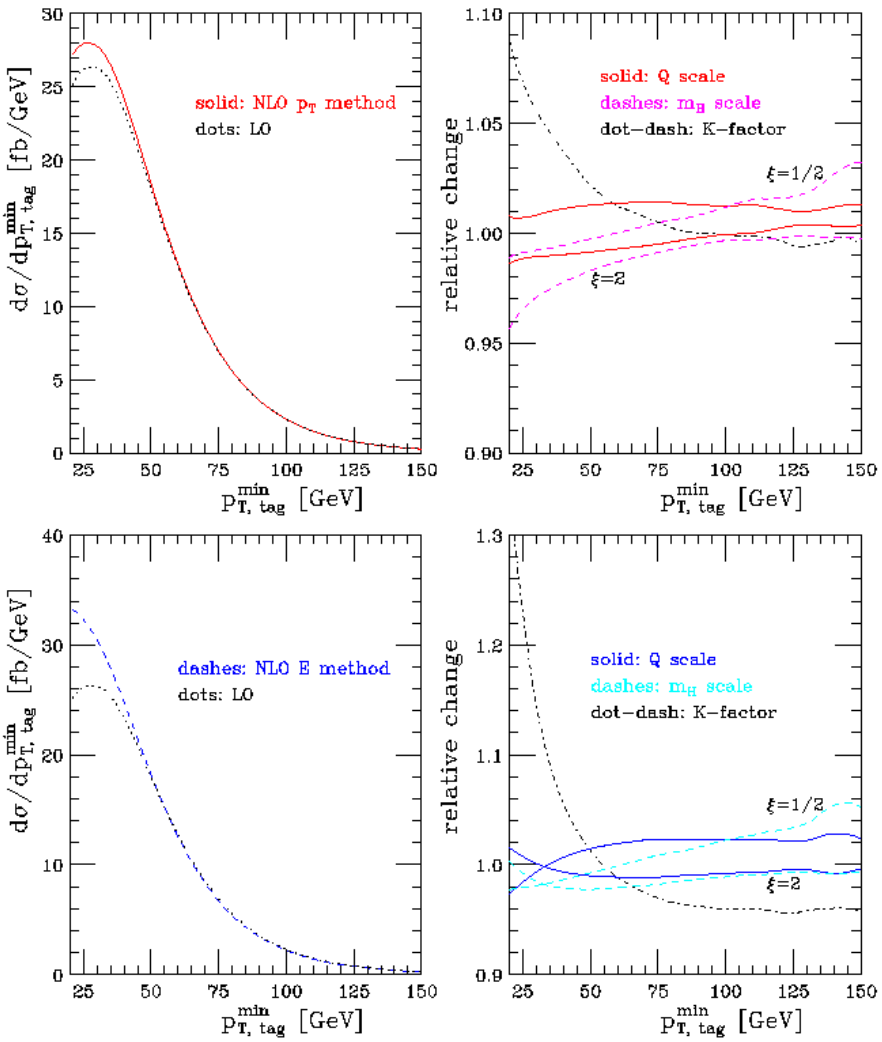

$$R = \frac{d\sigma^{NLO}(\mu_F = \mu_R = Q)}{d\sigma^{NLO}(\mu_F = \mu_R = \mu)}$$

- Tagging jets uniquely defined at LO
- Relatively large differences between p_T-method and E-method.
- The residual scale uncertainties:
  - -4% to $+2\%$ for p_T-method
  - -2% to $+5\%$ for E-method

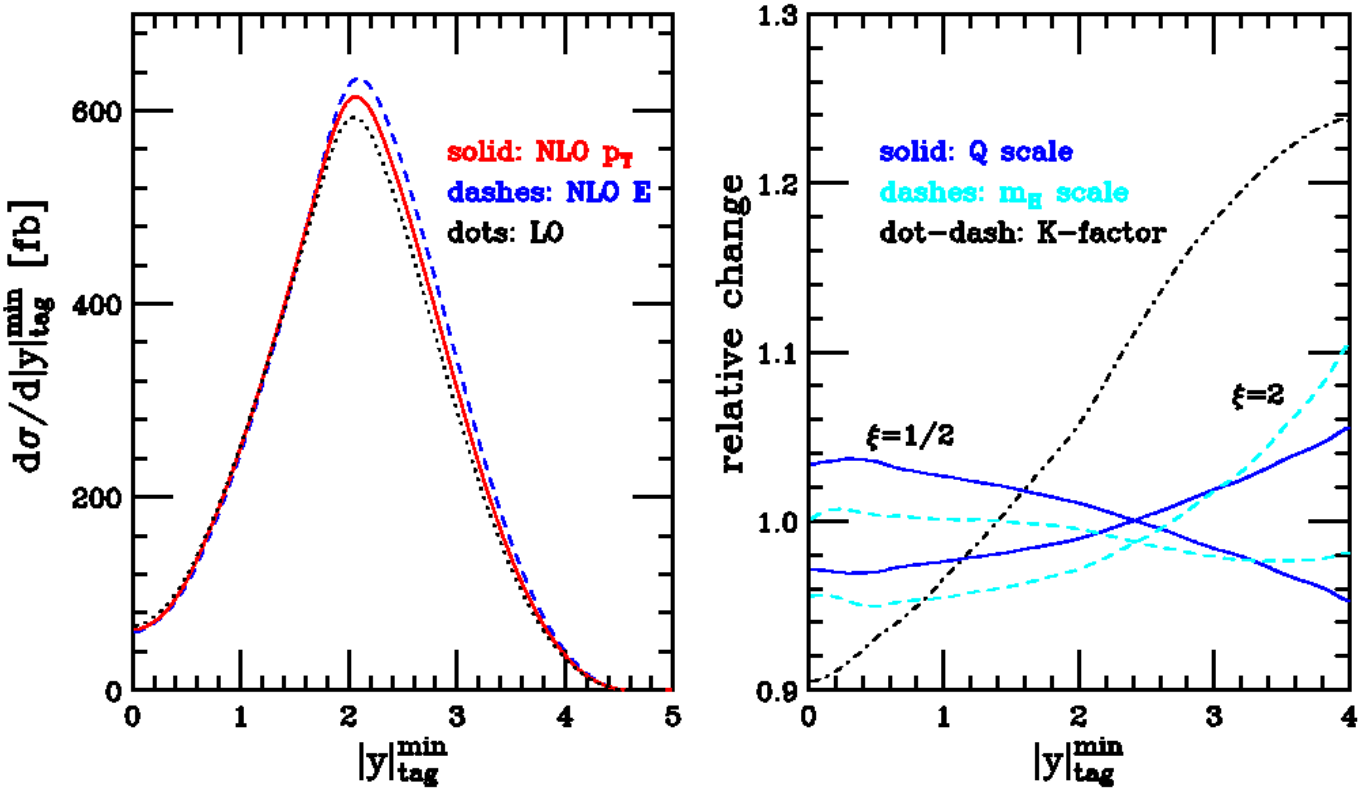

K-factor strongly phase-space dependent.

However, scale dependence is modest, in particular in the important region around $|y|^{min}_{tag} \approx 2$.

Scale variation below 4%.

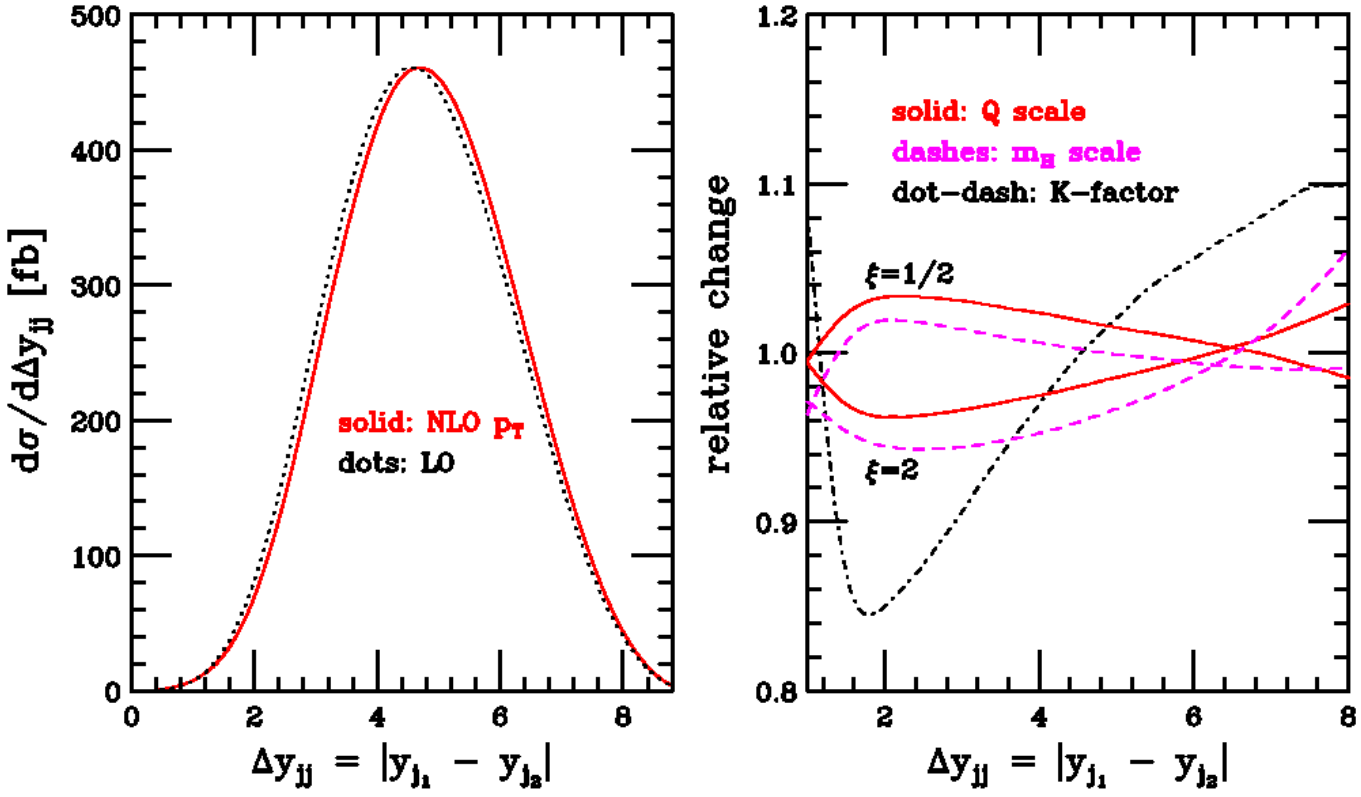

Tagging jets are slightly more forward at NLO than at LO

⇓

$\Delta y_{jj} > 4$ cut works well at NLO.

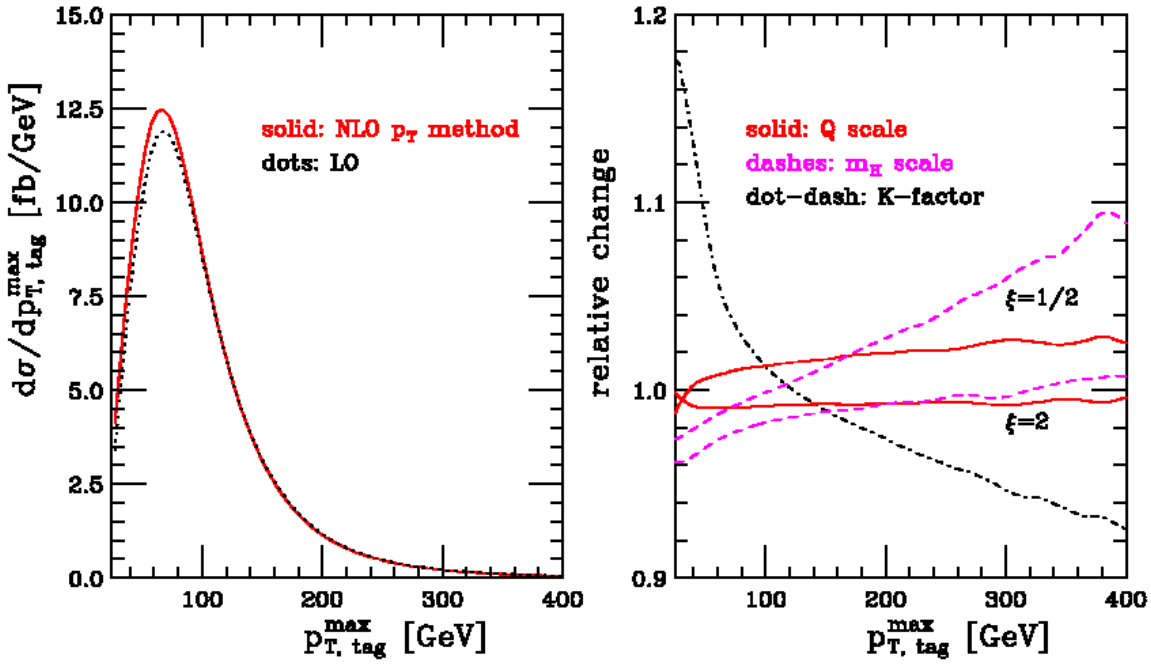

K-factor reaches 1.18

Scale variations:

- Increases to $+10\%$ at larger p_T for m_H scales.
- For Q_i scales staying in a narrow $\pm 2\%$ band.

The General Tensor Structure of the HVV Coupling

The most general tensor structure for HVV couplings for conserved quark currents is

$$\begin{aligned} T^{\mu\nu}(q_1,q_2) &= a_1(q_1,q_2)g^{\mu\nu} \\ &+ a_2(q_1,q_2)[q_1\cdot q_2 g^{\mu\nu} - q_2^\mu q_1^\nu] \\ &+ a_3(q_1,q_2)\varepsilon^{\mu\nu\rho\sigma}q_{1\rho}q_{2\sigma}\ . \end{aligned}$$

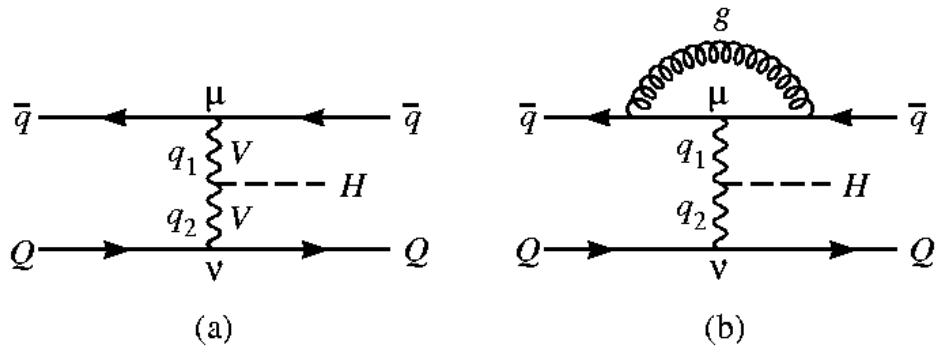

- SM-like HVV coupling: $a_1 = const.$
- CP even HVV coupling: a_2
- CP odd HVV coupling: a_3

To implement the general vertex in our NLO QCD Monte Carlo is straightforward since:

- $\mathcal{M}_V \propto \mathcal{M}_B$
- $\mathcal{M} \propto T_{\mu\nu} J_1^\mu J_2^\nu$

Couplings

The SM $g^{\mu\nu}$ coupling results from the kinetic energy term,

$$\begin{aligned}\mathcal{L}_K = (D_\mu\Phi)^\dagger(D^\mu\Phi) &= \frac{1}{4}g^2 W_\mu^+ W^{-\mu}(v+H)^2 \\ &+ \frac{1}{2}\partial_\mu H \partial^\mu H \\ &+ \frac{1}{8}g_Z^2 Z_\mu Z^\mu (v+H)^2\end{aligned}$$

for $\Phi \to (0,(v+H)/\sqrt{2})$

CP even and odd couplings are a result of the D5 operator:

$$\begin{aligned}\mathcal{L}_5 &= \frac{1}{\Lambda_{5e}} g_{5e}^{HWW} H W_{\mu\nu}^+ W^{-\mu\nu} \\ &+ \frac{1}{\Lambda_{5o}} g_{5o}^{HWW} H \tilde{W}_{\mu\nu}^+ W^{-\mu\nu} \\ &+ \frac{1}{2\Lambda_{5e}} g_{5e}^{HZZ} H Z_{\mu\nu} Z^{\mu\nu} \\ &+ \frac{1}{2\Lambda_{5o}} g_{5o}^{HZZ} H \tilde{Z}_{\mu\nu} Z^{\mu\nu}\end{aligned}$$

$\tilde{V}_{\mu\nu} = \frac{1}{2}\varepsilon_{\mu\nu\rho\sigma}V^{\rho\sigma}$

Feynman Rules

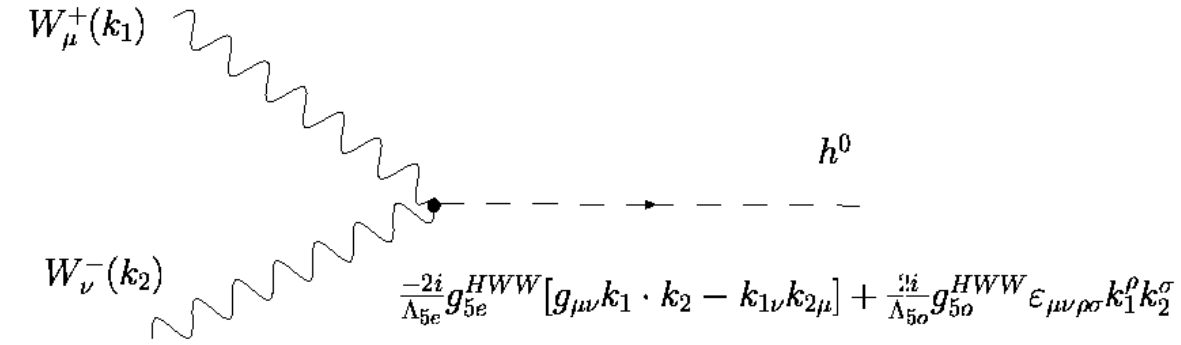

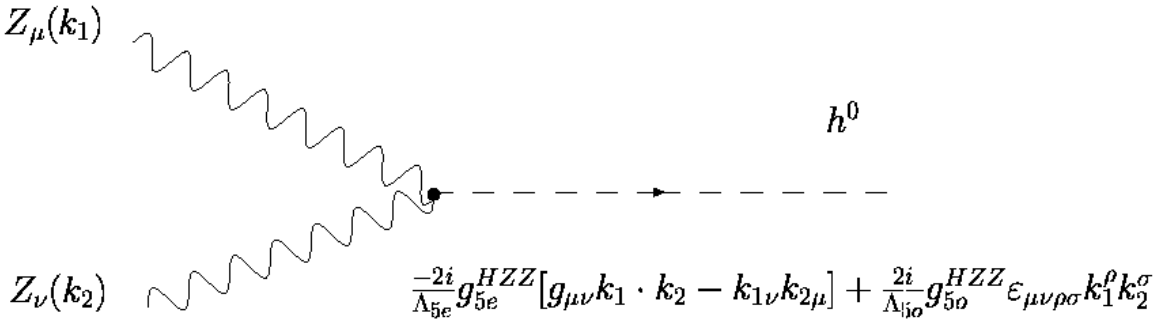

- CP even

$$g_{5o}^{HWW} = 0 \qquad g_{5e}^{HWW} = 1$$
$$g_{5o}^{HZZ} = 0 \qquad g_{5e}^{HZZ} = \frac{1}{\cos^2\theta_w}$$

- CP odd

$$g_{5e}^{HWW} = 0 \qquad g_{5o}^{HWW} = 1$$
$$g_{5e}^{HZZ} = 0 \qquad g_{5o}^{HZZ} = \frac{1}{\cos^2\theta_w}$$

$\Lambda_5 \simeq 480$ GeV reproduces the SM cross section.

Jet Correlations at LO

It has been pointed out * that the azimuthal angle correlations of the two quark jets in the WBF process $qQ \to qQH$ provide tell-tale signatures for the tensor structure of the HVV couplings:

- A flat distribution for the SM.
- For a $HV_{\mu\nu}V^{\mu\nu}$ coupling a pronounced dip at $\phi_{jj} = 90$ degrees.
- For a $H\tilde{V}_{\mu\nu}V^{\mu\nu}$ coupling a pronounced dip at $\phi_{jj} = 0$ and $\phi_{jj} = 180$ degrees.

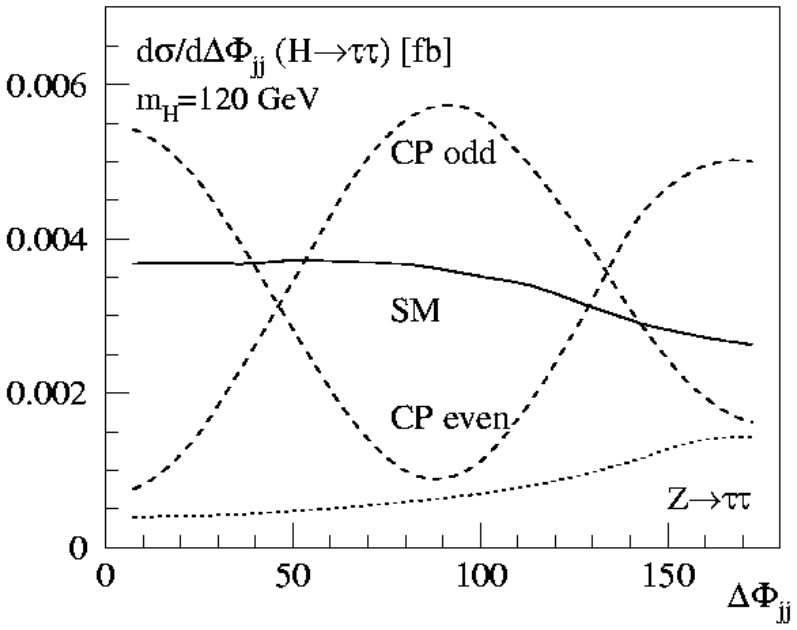

*T.Plehn,D.Rainwater,and D.Zeppenfeld,Phys.Rev.Lett.88,051801 (2001)

Jet Correlations at NLO

What happens to the azimuthal angle distributions of tagging jets when additional gluon emission is considered?

We address this question by modifying our NLO parton-level Monte Carlo program.

All cuts as stated earlier apply except that:

- do not simulate any Higgs decay
- $\mu_f = \mu_R = Q_i$
- $y_{j_1} \cdot y_{j_2} < 0$

Form factors and $d\sigma/dp_{Tj}(max)$

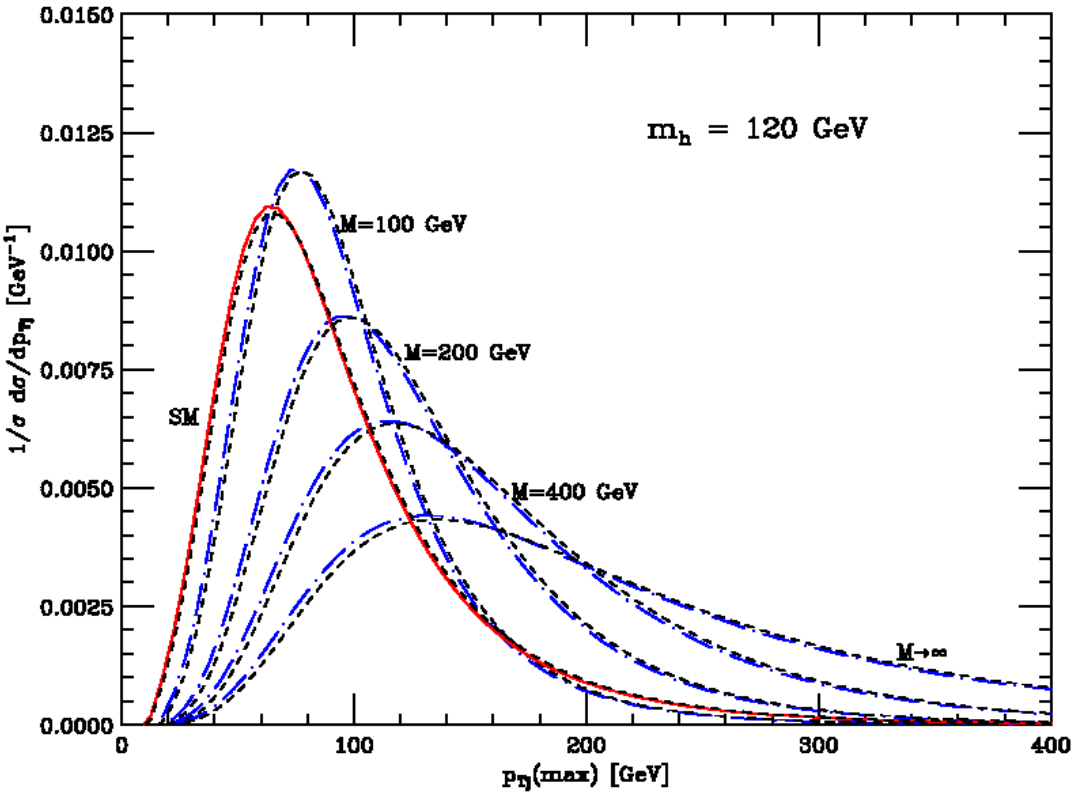

$$a_i(q_1, q_2) = a_i(0,0)\frac{M^2}{q_1^2 - M^2}\frac{M^2}{q_2^2 - M^2}$$

Anomalous couplings + form factors can mimic SM couplings!

Form factors and $d\sigma/d\phi_{jj}$

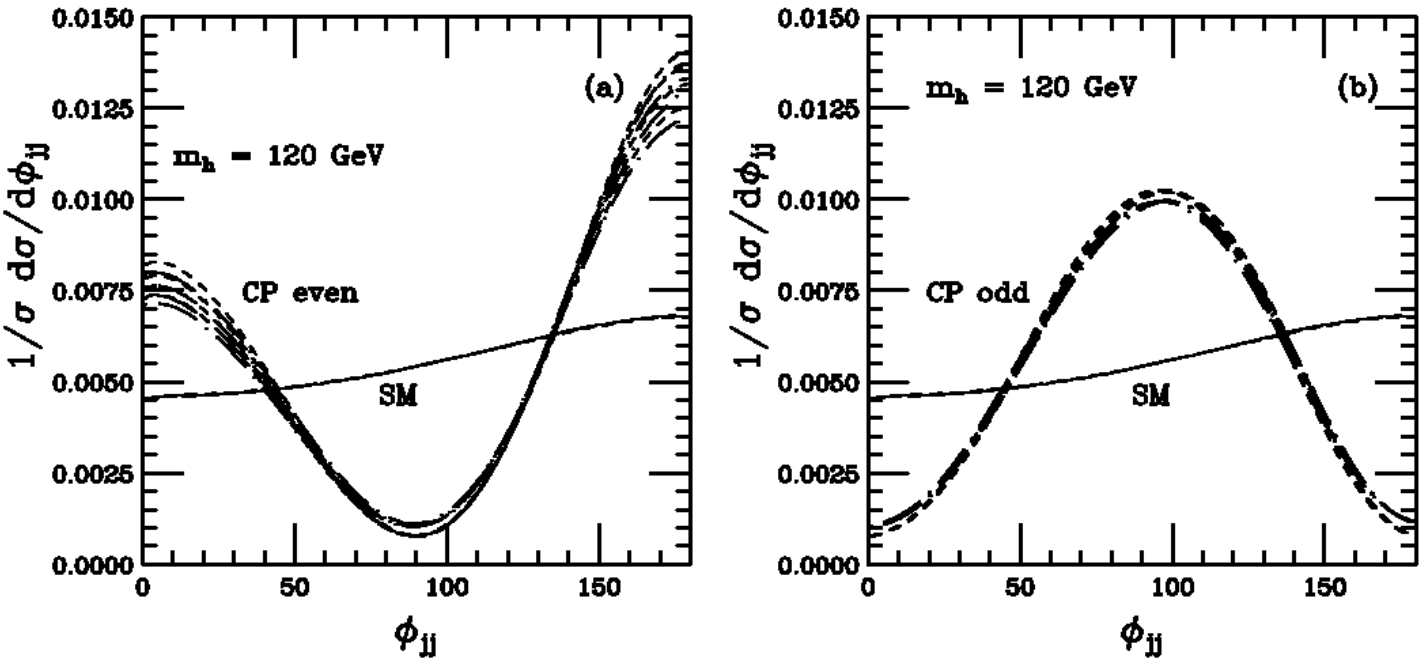

The form factor dependence is very small.

The dips in the CP even and CP odd coupling are clean signatures.

m_H dependence and $d\sigma/d\phi_{jj}$

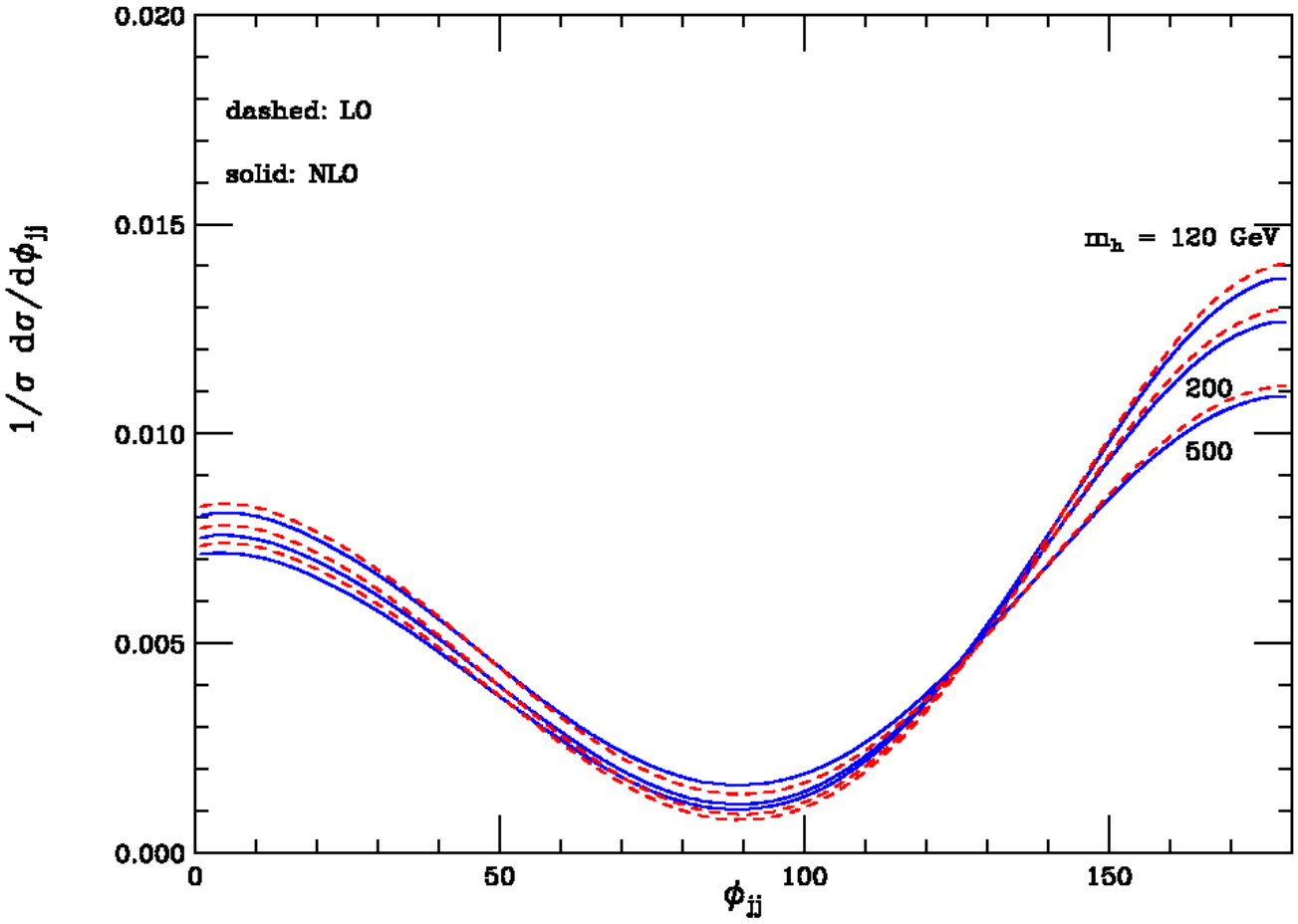

- NLO QCD corrections are small.
- No de-correlation of tagging jets.

Conclusions

- QCD corrections for WBF are strongly phase space dependent for jet observables and $K \cdot \sigma_{LO}$ is not an adequate approximation.
- K-factors and scale dependences are small in the Higgs boson search regions both for inclusive cross sections and distributions.
- Anomalous couplings lead to characteristic changes in the azimuthal angle correlations for the two tagging jets in WBF.
- The NLO QCD corrections do not de-correlate azimuthal angle correlations of the two tagging jets in WBF.